

5.1. Micromixing as Evolution of Concentration Moments.

Let us consider a fluid element of a diffusive tracer (spot of contaminant) being transported and deformed by surrounding liquid as it is shown in figure 5.1. The differential material balance for the tracer substance in Eulerian frame of reference (x_i, x_j) reads:

$$\frac{\partial c}{\partial t} + \sum_{i=1}^3 v_i \cdot \frac{\partial c}{\partial x_i} = D \cdot \sum_{i=1}^3 \frac{\partial^2 c}{\partial x_i^2} . \quad (5.2)$$

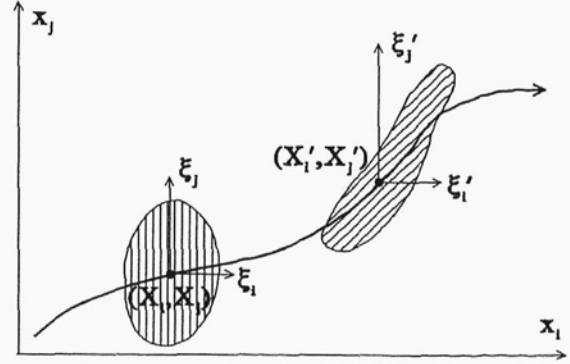


Figure 5.1. A drop of tracer liquid in an external flow field.

In the local coordinate system wandering with the fluid element the conservation equation becomes:

$$\frac{\partial c}{\partial t} + \sum_{i=1}^3 \frac{\partial}{\partial \xi_i} \{ c \cdot [v_i(\vec{\xi}) - v_i(\vec{0})] \} = D \cdot \sum_{i=1}^3 \frac{\partial^2 c}{\partial \xi_i^2} , \quad (5.3)$$

where ξ_i is the difference between Eulerian position x_i and the position of Lagrangian point X_i

$$\xi_i = x_i - X_i , \quad i = 1, 2, 3 . \quad (5.4)$$

The fluid element is assumed to be so small, that one can assume that within the fluid element and in its surrounding the velocity field is linear:

$$v_i(\vec{\xi}) = v_i(\vec{0}) + \sum_{j=1}^3 \xi_j \cdot \left. \frac{\partial v_i}{\partial \xi_j} \right|_{\vec{0}} , \quad i = 1, 2, 3 . \quad (5.5)$$

Thus substitution of equation (5.5) into equation (5.3) yields:

$$\frac{\partial c}{\partial t} + \sum_{i=1}^3 \sum_{j=1}^3 \xi_j \cdot \frac{\partial v_i}{\partial \xi_j} \cdot \frac{\partial c}{\partial \xi_i} = D \cdot \sum_{i=1}^3 \frac{\partial^2 c}{\partial \xi_i^2} . \quad (5.6)$$

Following Tennekes and Lumley [72] and treating concentration of the tracer substance as a three-dimensional probability density function one can characterize the shape of the spot by concentration moments:

$$I_{kl} = \int \int \int_{-\infty}^{+\infty} \xi_k \cdot \xi_l \cdot c \, d\xi_1 d\xi_2 d\xi_3 \bigg/ \int \int \int_{-\infty}^{+\infty} c \, d\xi_1 d\xi_2 d\xi_3 . \quad (5.7)$$

In this case, the diagonal moments I_{ii} are related to the spot shape defined by penetration distances δ_i (as shown in figure 5.2) by:

$$\delta_1^2 : \delta_2^2 : \delta_3^2 = I_{11} : I_{22} : I_{33} . \quad (5.8)$$

Integration of material balance (5.6) with weight functions $\xi_k \cdot \xi_l$ leads to the system of ordinary differential equations:

$$\frac{dI_{kl}}{dt} - \sum_{j=1}^3 \left(\frac{\partial v_j}{\partial \xi_j} \cdot I_{kl} + \frac{\partial v_l}{\partial \xi_j} \cdot I_{kj} + \frac{\partial v_k}{\partial \xi_j} \cdot I_{lj} \right) = 2 \cdot D \cdot \delta_{kl} , \quad (5.9)$$

where

$$\delta_{kl} = \begin{cases} 1 & \text{if } k=l \\ 0 & \text{if } k \neq l \end{cases} . \quad (5.10)$$

If the axes of Lagrangian frame are coincident with the main axes of deformation then off-diagonal components of velocity gradient tensor are equal to zero:

$$\frac{\partial v_i}{\partial \xi_j} = \begin{cases} \alpha_i \neq 0 & \text{if } i=j \\ 0 & \text{if } i \neq j \end{cases} , \quad (5.11)$$

where α_i is a deformation rate in i direction. On the other hand, the condition of continuity requires:

$$\alpha_1 + \alpha_2 + \alpha_3 = 0 . \quad (5.12)$$

Substitution of (5.11) into (5.9) while taking into account (5.12) yields:

$$\frac{dI_{ii}}{dt} - 2 \cdot \alpha_i \cdot I_{ii} = 2 \cdot D , \quad i=1,2,3 . \quad (5.13)$$

which finally gives for $\alpha_i = \text{const}$

$$I_{ii}(t) = \left(I_{ii}(0) + \frac{D}{\alpha_i} \right) \cdot e^{2\alpha_i t} - \frac{D}{\alpha_i} , \quad i=1,2,3 . \quad (5.14)$$

Expression (5.14) describes evolution of diagonal moments in time. For $\alpha_3=0$ the flow can be characterized by a single parameter (see discussion in chapter 2)

$$\alpha = -\alpha_1 = \alpha_2 . \quad (5.15)$$

Analysis of equation (5.14) shows that when $\alpha > 0$ concentration moment I_{11} and consequently

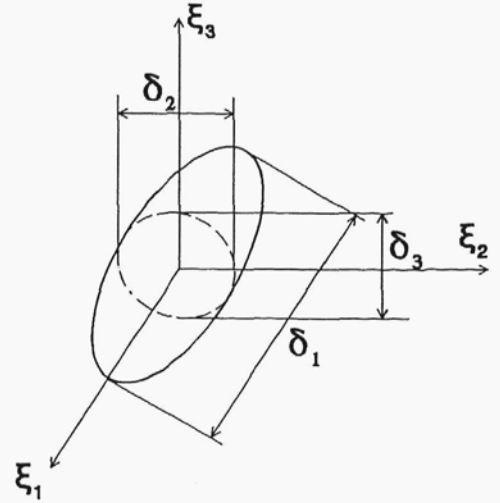


Figure 5.2. Spatial characterization of the drop of tracer solution.

the penetration distance δ_1 stabilize for times longer than $1/\alpha$

$$\delta_1(\infty) \sim \sqrt{I_{11}(\infty)} = \sqrt{D/\alpha} , \quad (5.16)$$

in agreement with earlier findings; compare equation (5.16) with equation (3.35). It should be pointed out that the limiting penetration distance $\delta_1(\infty)$ as well as the universal normalized profile (3.34) do not depend on the initial distribution of the tracer substance. Expression (5.14) allows to estimate the volume of liquid containing the tracer substance

$$V/V_0 = \sqrt{I_{11}(t) \cdot I_{22}(t) \cdot I_{33}(t)} / \sqrt{I_{11}(0) \cdot I_{22}(0) \cdot I_{33}(0)} . \quad (5.17)$$

and the relative rate of growth of this volume

$$\frac{1}{V} \cdot \frac{dV}{dt} = \frac{1}{2} \cdot \sum_{i=1}^3 \frac{1}{I_{ii}} \cdot \frac{dI_{ii}}{dt} . \quad (5.18)$$

Substituting equations (5.12) and (5.14) into (5.18) one has:

$$\frac{1}{V} \cdot \frac{dV}{dt} = \sum_{i=1}^3 \frac{D}{I_{ii}} = \sum_{i=1}^3 \left[(I_{ii}(0)/D + 1/\alpha_i) \cdot e^{2\alpha_i t} - 1/\alpha_i \right]^{-1} . \quad (5.19)$$

Analysis of equation (5.19) shows that in very viscous liquids where $D \ll 1$, the volume of the spot of the tracer does not change in time initially (i.e. for $t \ll 1/\alpha$), whereas for times longer than $1/\alpha$ this volume grows exponentially. In the case: $-\alpha_1 = \alpha_2 = \alpha$, $\alpha_3 = 0$ one has

$$\lim_{t \rightarrow \infty} \frac{1}{V} \cdot \frac{dV}{dt} = \alpha . \quad (5.20)$$

Let us consider now a slab of contaminant deformed in a two-dimensional stagnation flow, as shown in figure 3.2. Because $(\partial c / \partial \xi_2 = \partial c / \partial \xi_3 = 0)$, equations (5.17) and (5.19) can be reduced to:

$$V/V_0 = \sqrt{I_{11}(t)/I_{11}(0)} \cdot e^{\alpha t} , \quad (5.21)$$

$$\frac{1}{V} \cdot \frac{dV}{dt} = \frac{D}{I_{11}} = \left[(I_{11}(0)/D - 1/\alpha) \cdot e^{-2\alpha t} + 1/\alpha \right]^{-1} . \quad (5.22)$$

Similar analysis can be performed assuming that the flow in the close proximity of the drop of tracer solution is axisymmetric, i.e:

$$v_r = -\alpha \cdot r/2 , \quad v_\theta = 0 , \quad v_z = \alpha \cdot z . \quad (3.36)$$

Neglecting tangential variation of the tracer concentration in the differential balance equation

one has:

$$\frac{\partial c}{\partial t} - \frac{\alpha \cdot r}{2} \cdot \frac{\partial c}{\partial r} + \alpha \cdot z \cdot \frac{\partial c}{\partial z} = D \cdot \left[\frac{1}{r} \cdot \frac{\partial}{\partial r} \left(r \cdot \frac{\partial c}{\partial r} \right) + \frac{\partial^2 c}{\partial z^2} \right] \quad (5.23)$$

The radial and axial penetration distances can be estimated as the square roots of moments I_{rr} and I_{zz} :

$$I_{rr} = \int_{-\infty}^{+\infty} \int_0^{+\infty} r^2 \cdot c \cdot 2 \cdot \pi \cdot r dr dz \bigg/ \int_{-\infty}^{+\infty} \int_0^{+\infty} c \cdot 2 \cdot \pi \cdot r dr dz, \quad (5.24a)$$

$$I_{zz} = \int_{-\infty}^{+\infty} \int_0^{+\infty} z^2 \cdot c \cdot 2 \cdot \pi \cdot r dr dz \bigg/ \int_{-\infty}^{+\infty} \int_0^{+\infty} c \cdot 2 \cdot \pi \cdot r dr dz. \quad (5.24b)$$

Integration of equation (5.23) with suitable weight functions gives the moments equations:

$$\frac{dI_{rr}}{dt} + \alpha \cdot I_{rr} = 4 \cdot D, \quad (5.25a)$$

$$\frac{dI_{zz}}{dt} - 2 \cdot \alpha \cdot I_{zz} = 2 \cdot D. \quad (5.25b)$$

For the case $\alpha = \text{const}$ one receives:

$$I_{rr}(t) = \left(I_{rr}(0) - \frac{4 \cdot D}{\alpha} \right) \cdot e^{-\alpha t} + \frac{4 \cdot D}{\alpha}. \quad (5.26a)$$

$$I_{zz}(t) = \left(I_{zz}(0) + \frac{D}{\alpha} \right) \cdot e^{2\alpha t} - \frac{D}{\alpha}. \quad (5.26b)$$

Notice that the value of $\sqrt{I_{rr}}$ and consequently the radial penetration distance tends in time to a limit:

$$\delta_r(\infty) \sim \sqrt{I_{rr}(\infty)} = 2 \cdot \sqrt{D/\alpha} \quad (5.27)$$

The volume of the spot containing the tracer can be estimated as:

$$V/V_0 = [I_{rr}(t)/I_{rr}(0)] \cdot \sqrt{I_{zz}(t)/I_{zz}(0)}, \quad (5.28)$$

whereas the rate of growth of the spot is given by

$$\frac{1}{V} \cdot \frac{dV}{dt} = \frac{1}{I_{rr}} \cdot \frac{dI_{rr}}{dt} + \frac{1}{2 \cdot I_{zz}} \cdot \frac{dI_{zz}}{dt} = D \cdot \left(\frac{4}{I_{rr}} + \frac{1}{I_{zz}} \right). \quad (5.29)$$

If instead of the spot, an elongated filament is considered then $\partial c / \partial z = 0$ and equations (5.28)

and (5.29) become:

$$V(t)/V(0) = [I_{rr}(t)/I_{rr}(0)] \cdot e^{\alpha t}, \quad (5.30)$$

$$\frac{1}{V} \cdot \frac{dV}{dt} = \frac{4 \cdot D}{I_{rr}(t)} = \left\{ [I_{rr}(0)/(4 \cdot D) - 1/\alpha] \cdot e^{-\alpha t} + 1/\alpha \right\}^{-1}. \quad (5.31)$$

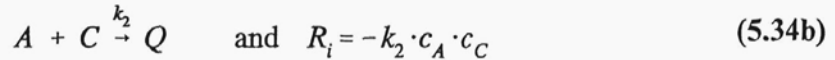
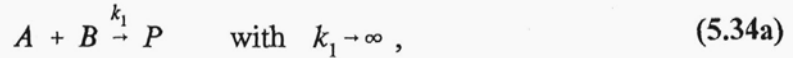
When mixing is accomplished by a chemical reaction, expressions of type (5.19) and (5.29) can be used to formulate material balances of reactants. Let c_i be the average concentration of reactant i in the reaction zone and let $\langle c_i \rangle$ be the concentration of the reactant i in the environment. The material balance reads in this case:

$$\frac{d}{dt}(V \cdot c_i) = V \cdot R_i + \frac{dV}{dt} \cdot \langle c_i \rangle, \quad (5.32)$$

where R_i is the reaction rate. Rearrangement of equation (5.32) gives

$$\frac{dc_i}{dt} = \frac{1}{V} \cdot \frac{dV}{dt} \cdot (\langle c_i \rangle - c_i) + R_i. \quad (5.33)$$

To illustrate the model application, let us consider a system of competitive-parallel reactions of the second order:



carried out in the system shown in figure 5.3. Concentrated solution of A is slowly fed into the premixture of B and C. The chemically equivalent amounts of A, B and C are applied, i.e.

$$V_{A0} \cdot c_{A0} = V_{(B,C)0} \cdot c_{B0} = V_{(B,C)0} \cdot c_{C0}. \quad (5.35)$$

For instantaneous mixing the limiting substrate A should be consumed in the instantaneous reaction with reactant B. For slower mixing some A should be consumed in the reaction with C due to local inhomogeneity. Slower mixing results in more A consumed in the second reaction. Thus, the state of mixedness can be uniquely defined by the final selectivity [66,73]:

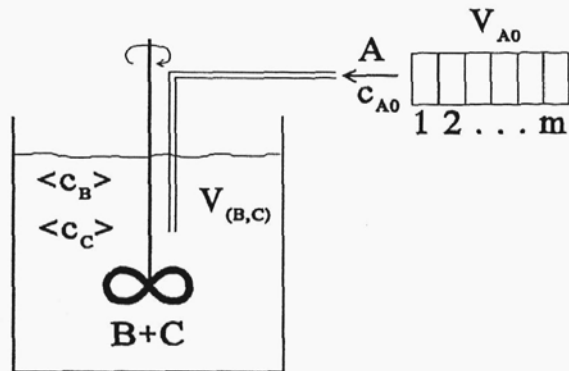


Figure 5.3. A semi-batch reactor.

$$X = \Delta N_C / N_{A0} . \quad (5.36)$$

Notice that in the case of perfect mixedness on the molecular scale $X=0$, whereas in the case when both reactions are mixing controlled $X=0.5$.

Depending on the flow pattern in the reactor, the position of a feeding point and the feeding rate, the stream of A-rich solution may take different shapes, e.g. a slab or a filament. In the case when feeding is so slow that the inlet stream is swept from the tip of the feeding pipe, one can assume that the feeding stream forms a thin ribbon which is afterwards elongated. If the reactant A is introduced into the reactor by a small pipe having a circular outlet then for high feeding rates, one can assume that A-rich liquid forms a cylindrical thread elongated during mixing, as shown in figure

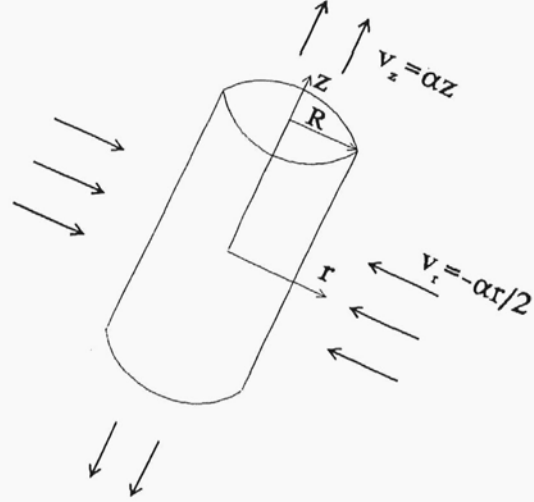


Figure 5.4. Translating and rotating filament in a local Lagrangian coordinate system.

5.4. The method of integral concentration moments allows to model micromixing in Lagrangian frame of reference in both cases. When the feeding stream forms the slab then relations (5.21) and (5.22) should be used. On the other hand, if the feeding stream forms a filament then relations (5.30) and (5.31) should be applied.

Semibatch operation is simulated by discretizing the feed addition into m equal parts of volume

$$V_0 = V_{A0} / m , \quad (5.37)$$

similarly as in [66,73]. The material balance equations (5.33) written for reactants A and C become:

$$\frac{dc_A}{dt} = -\frac{1}{V} \cdot \frac{dV}{dt} \cdot (c_A + \langle c_B \rangle) - k_2 \cdot c_A \cdot c_C , \quad (5.38a)$$

$$\frac{dc_C}{dt} = -\frac{1}{V} \cdot \frac{dV}{dt} \cdot (c_C - \langle c_C \rangle) - k_2 \cdot c_A \cdot c_C \quad (5.38b)$$

with initial conditions given by:

$$V(0) = V_0 , \quad c_A(0) = c_{A0} , \quad c_C(0) = 0 . \quad (5.38c)$$

The initial composition of **B** and **C** solution is

$$\langle c_A \rangle = 0, \quad \langle c_B \rangle = c_{B0}, \quad \langle c_{C0} \rangle = c_{C0}. \quad (5.39)$$

The product distribution is computed when the reaction has run to completion and $c_A = 0$. The volume of the reaction zone starts at V_0 and develops to the volume calculated either from equation (5.21) or from equation (5.30); for the time until **A** has been fully consumed.

Using m equal parts of V_{A0} , $\langle c_B \rangle$ and $\langle c_C \rangle$ can be updated as follows. The k -th part of the feed ($1 \leq k \leq m$) reacts in time t_{fk} . The surroundings, therefore, have the volume $V_{(B,C)0} + k \cdot V_0$ and the concentrations are:

$$\langle c_B \rangle_k = \langle c_B \rangle_{k-1} \cdot \left[1 - \frac{V(t_{fk})}{V_0} \cdot \frac{V_0}{V_{(B,C)0} + k \cdot V_0} \right], \quad (5.40a)$$

$$\langle c_C \rangle_k = \langle c_C \rangle_{k-1} + [c_C(t_{fk}) - \langle c_C \rangle_{k-1}] \cdot \frac{V(t_{fk})}{V_0} \cdot \frac{V_0}{V_{(B,C)0} + k \cdot V_0}. \quad (5.40b)$$

These concentrations refer to the surroundings during the next $(k+1)$ part of the feed. The system of equations (5.38)÷(5.40) and either (5.21)÷(5.22) or (5.30)÷(5.31) can be expressed using dimensionless variables and parameters:

$$\text{– dimensionless concentration} \quad C_i = c_i / c_{A0}, \quad (5.41a)$$

$$\text{– dimensionless time} \quad \Gamma = t / t_F, \quad (5.41b)$$

$$\text{– Damköhler number} \quad Da = k_2 \cdot c_{A0} \cdot t_D, \quad (5.42a)$$

$$\text{– volume ratio} \quad a = V_{(B,C)0} / V_{A0}, \quad (5.42b)$$

$$\text{– stoichiometric ratios} \quad F_B = N_{B0} / N_{A0}, \quad F_C = N_{C0} / N_{A0}, \quad (5.42c)$$

$$\text{– characteristic time ratio} \quad \theta = t_D / t_F. \quad (5.42d)$$

The characteristic deformation time t_F equals $1/\alpha$, whereas the characteristic diffusion time is related to the initial penetration distance, δ_0 :

$$t_D = \delta_0^2 / D_A. \quad (5.43)$$

The relation between δ_0 and the initial thickness of the slab of **A**-rich solution s_0 can be found from (5.7):

$$\delta_0 = \sqrt{I_{11}(0)} = s_0/\sqrt{12} . \quad (5.44)$$

If the feeding stream has a filament shape of initial radius R_0 then δ_0 can be found from (5.24a):

$$\delta_0 = \sqrt{I_{rr}(0)} = R_0/\sqrt{2} . \quad (5.45)$$

The governing equations (5.38)÷(5.40) written in dimensionless form become:

$$\frac{dC_A}{d\Gamma} = -\psi \cdot (C_A + \langle C_B \rangle) - \frac{Da}{\theta} \cdot C_A \cdot C_C , \quad (5.46a)$$

$$\frac{dC_B}{d\Gamma} = -\psi \cdot (C_C - \langle C_C \rangle) - \frac{Da}{\theta} \cdot C_A \cdot C_C , \quad (5.46b)$$

$$\Gamma=0 , \quad C_A=1 , \quad C_C=0 , \quad (5.46c)$$

where

$$\psi = [(\theta/j^2 - 1) \cdot e^{-2\Gamma/lj} + 1]^{-1} \quad (5.47)$$

and

$$\langle C_B \rangle_0 = F_B/a , \quad \langle C_C \rangle_0 = F_C/a , \quad (5.48a)$$

$$\langle C_B \rangle_k = \langle C_B \rangle_{k-1} \cdot \left\{ 1 - \left[1 + \frac{j^2}{\theta} \cdot (e^{2\Gamma_{fk}/lj} - 1) \right]^{j/2} / (m \cdot a + k) \right\} , \quad (5.48b)$$

$$\langle C_C \rangle_k = \langle C_C \rangle_{k-1} + [C_C(\Gamma_{fk}) - \langle C_C \rangle_{k-1}] \cdot \left[1 + \frac{j^2}{\theta} \cdot (e^{2\Gamma_{fk}/lj} - 1) \right]^{j/2} / (m \cdot a + k) . \quad (5.48c)$$

In equations (5.47) and (5.48) $j=1$ is appropriate for the slab, whereas $j=2$ is appropriate for the filament.

Instead of relating Damköhler number to feed concentration c_{A0} , one can define Damköhler number using average concentration \bar{c}_{A0} :

$$\overline{Da} = k_2 \cdot \overline{c_{A0}} \cdot t_D = k_2 \cdot \frac{c_{A0}}{a+1} \cdot t_D . \quad (5.49)$$

The average concentration \bar{c}_{A0} is the concentration which reagent A would have if all of it had been added to the reactor and well mixed before reacting. Definition (5.49) enables direct comparison of product distributions obtained for different volume ratios but for the same number of reactant moles.

Discretization m of the feed, which appears in global stoichiometric balances (5.48) should be high enough not to affect the final product selectivity. Table 5.I shows that when m is higher than 100 the effect of increase of m becomes negligible. Thus, the degree of discretization is set to 100.

Table 5.I. Effect of the feed discretization on selectivity;
 $Da=100$, $\theta=1000$, $a=100$, $F_B=F_C=1$.

m		10	20	50	100	200	500
X[%]	slab	14.47	14.64	14.74	14.78	14.79	14.80
	filament	14.76	14.92	15.03	15.06	15.08	15.09

Another important model parameter is the length scale δ_0 , which is directly proportional to the initial values of the slab thickness - equation (5.44) or the filament radius - equation (5.45). On the other hand, the time ratio, θ , and Damköhler number, \overline{Da} , are both proportional to the square of δ_0 . Thus, to find the effect of δ_0 on the product distribution X , one has to change simultaneously \overline{Da} and θ while keeping the ratio \overline{Da}/θ constant. Such an analysis was performed for $\overline{Da}/\theta=0.1$ and for four different values of volume ratio a . The results of model predictions, presented in figures 5.5ab, indicate that there is a region of δ_0 where the selectivity is strongly dependent on δ_0 . Effects of δ_0 are negligible for very small δ_0 , where diffusional mixing is al-

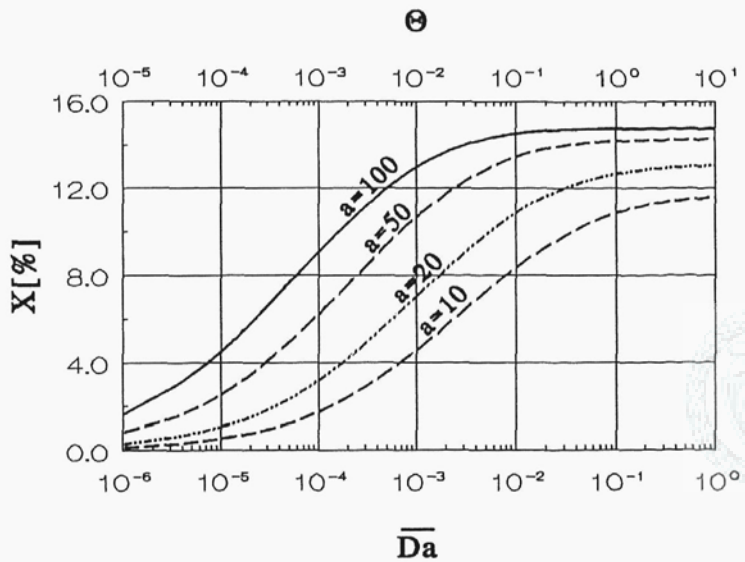


Figure 5.5a. Effect of δ_0 and a on selectivity; feeding stream has a slab shape, $F_B=F_C=1$.

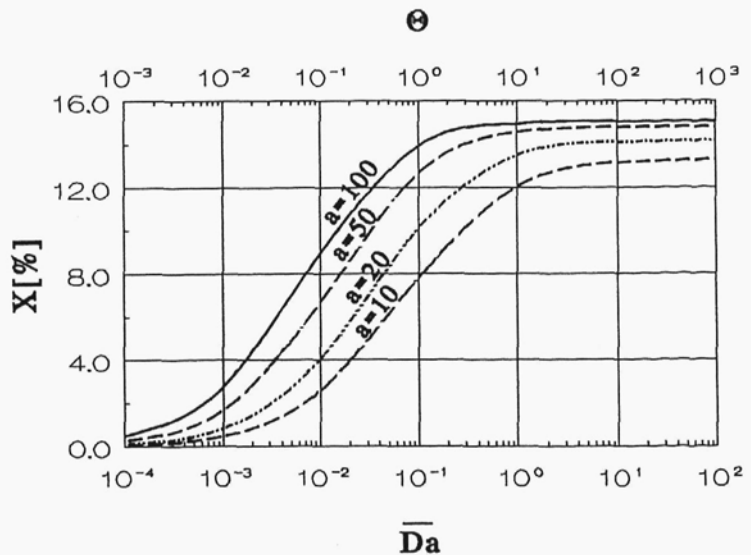


Figure 5.5b. Effect of δ_0 and a on selectivity; feeding stream has a filament shape, $F_B=F_C=1$.

most instantaneous and for very large δ_0 where diffusional mixing is negligible. Comparison of figures 5.5ab shows that when the feeding stream has a slab shape then the effect of δ_0 on X is detectable for larger values of δ_0 than in the case when the feeding stream has a filament shape. This is so, because in simple stagnation flow (figure 3.2) the rate of growth of the reaction zone is less influenced by molecular diffusion than in the axi-symmetric flow (figure 5.4) - compare relations (5.22) and (5.31).

Figures 5.5ab illustrate also influence of the initial volume ratio a on the product distribution. This effect is weaker in the region where X does not depend on δ_0 than in the region where X depends on δ_0 . It should be noticed that in all cases decreasing the volume ratio improves mixing. This is so, because when a more concentrated portion of A-rich solution is fed into the reactor, it takes more time before reagent A is consumed, than in the case when a less concentrated A-rich solution is fed into the reactor. The longer mixing times, the higher chances for the slower reaction to proceed and elevate the final selectivity.

Very highly sensitivity of X to θ was found when \overline{Da} was kept constant. Figures 5.6ab show several curves obtained for θ ranging from 100 to 10^5 . As expected, increasing of θ (equivalent to faster mixing) always decreases the selectivity. Increasing of \overline{Da} increases selectivity due to decrease of the characteristic reaction time $t_R = 1/(k_2 \cdot c_{A0})$ of the second reaction. It should also be noted, that the final selectivities obtained for the same values of \overline{Da} and θ but for dif-

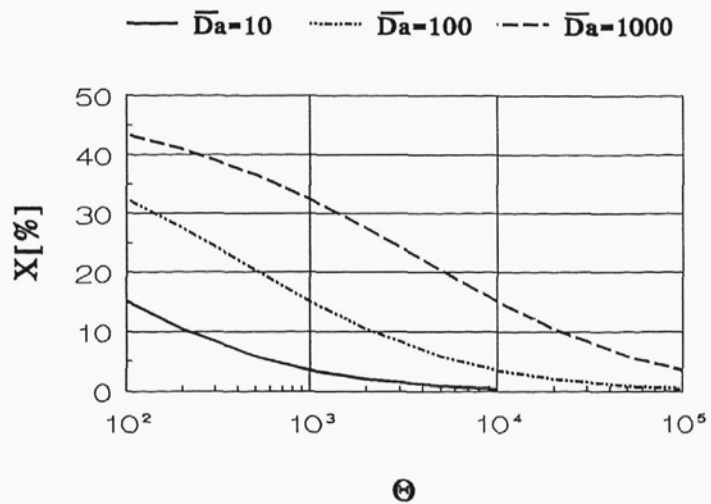


Figure 5.6a. Effect of θ on selectivity; feeding stream has a slab shape, $F_B=F_C=1$, $a=100$.

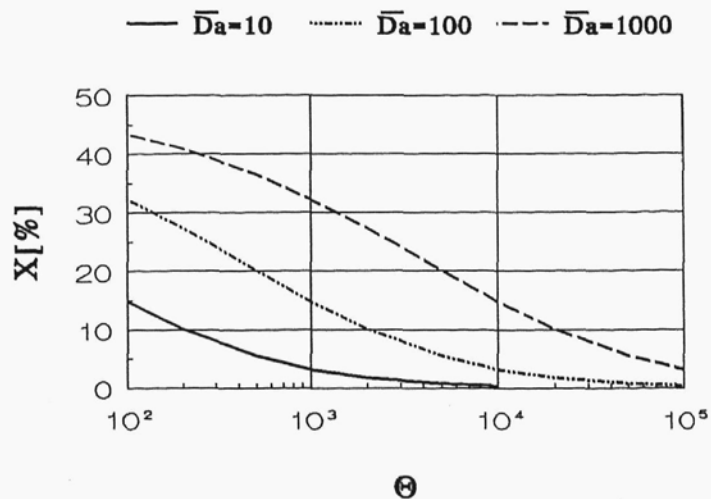


Figure 5.6b. Effect of θ on selectivity; feeding stream has a filament shape, $F_B=F_C=1$, $a=100$.

ferent shapes of the feeding stream are very close. Considering the fact that the computations were performed in the region where \mathbf{X} does not depends on δ_0 , it shows that the shape of the feeding stream can affect the product distribution only for very slow feeding rates.

One can conclude that the proposed model of micromixing enables prediction of influence of main processing parameters such as $\overline{\mathbf{Da}}$, θ , \mathbf{a} and \mathbf{F}_i on the course of mixing and reaction. The model gives also the possibility to relate the shape and size of the reaction zone to the product distribution. Contrary to the lamellar structure model [22,23], the present approach takes into account not only mixing within separated fluid elements but also mass exchange between the fluid elements and their surrounding. This is due to the fact that the volume of the reaction zone grows because of molecular diffusion, accelerated by deformation. However, it should be pointed out that the model relates the growth of the volume of the reaction zone only to the diffusion coefficient of the reactant initially contained in the reaction zone. Thus, the model estimations are correct provided that an initial concentration of this reactant is much higher than the concentrations of other reactants in the environment.

5.2. An Integral Method for Mixing and Chemical Reaction in Deformed Diffusion Layers.

When mixing in a local frame of reference proceeds between species reacting instantaneously, the reaction zone is reduced to a plane and the process is completely controlled by molecular diffusion. In the case of single irreversible reaction



one has to solve the system of two equations of type:

$$\frac{\partial c_i}{\partial t} - \alpha \cdot x \frac{\partial c_i}{\partial x} = D_i \cdot \frac{\partial^2 c_i}{\partial x^2} \quad (5.51a)$$

with the condition linking species fluxes at the reaction plane:

$$\nu_A \cdot D_A \frac{\partial c_A}{\partial x} + \nu_B \cdot D_B \cdot \frac{\partial c_B}{\partial x} = 0 \quad (5.51b)$$

Solution of equations (5.51) is difficult due to the presence of the moving boundary. Only in a specific case $\mathbf{D}_A = \mathbf{D}_B$ can system (5.51) be reduced to

$$\frac{\partial c}{\partial t} - \alpha \cdot x \frac{\partial c}{\partial x} = D \cdot \frac{\partial^2 c}{\partial x^2} \quad (5.52)$$